

The properties of the Higgs bosons and Pair Production of the SM-like Higgs Boson in λ -SUSY at the LHC

Haijing Zhou¹, Zhaoxia Heng¹, Dongwei Li²

¹*Department of Physics, Henan Normal University, Xinxiang 453007, China*

²*Department of Foundation, Henan Police College, Zhengzhou 450000, China*

Abstract

Compared with the MSSM or the NMSSM with a low λ , λ -SUSY theory with a large λ around one has been deemed as a most natural realization of NMSSM. In this work, we treat the next-to-lightest CP-even Higgs boson as the SM-like Higgs boson in λ -SUSY and study the properties of the Higgs bosons and the pair production of the SM-like Higgs boson by considering various experiment constraints. We find that naturalness plays an important role in selecting the parameter space of λ -SUSY. In the most natural region of parameter space, the triple self coupling of the SM-like Higgs boson compared with its SM prediction may get enhanced by a factor about 7, and the most dominant contribution to the Higgs pair production comes from the triple self coupling of the SM-like Higgs boson and the production rate can be greatly enhanced, maximally 10 times larger than the SM prediction.

PACS numbers: 14.80.Da,12.60.Jv

I. INTRODUCTION

Since a near 125 GeV scalar particle was discovered in 2012, both the ATLAS and CMS collaborations have accumulated overwhelming evidence [1–4] and the experimental data manifest that the properties of this new particle are roughly coincident with the Higgs boson predicted by the Standard Model (SM). However, it is yet unclear whether this particle is the Higgs boson in the SM. Moreover, the slight excess of the di-photon signal rate for the 125 GeV scalar reported by the LHC experiment [5, 6] can be interpreted reasonably in new physics models, such as the Minimal Supersymmetric Standard Model (MSSM) [7–11] and the Next-to-Minimal Supersymmetric Model (NMSSM) [12–23]. Although the MSSM can accommodate a 125 GeV Higgs boson, it needs sizable radiative corrections from top/stop loops, which will lead to some fine-tuning and seems unnatural. As the simplest realization of non-minimal extension of SUSY at the weak scale, NMSSM can offer additional contributions to the tree-level Higgs mass, which are not present in the MSSM, to accommodate a 125 GeV Higgs with significantly less fine-tuning.

Compared with the particle content of the MSSM, the NMSSM adds an additional gauge singlet superfield \hat{S} . Consequently, the form of its superpotential is given by[21–23]:

$$W^{\text{NMSSM}} = W_F + \lambda \hat{H}_u \cdot \hat{H}_d \hat{S} + \frac{1}{3} \kappa \hat{S}^3, \quad (1)$$

with W_F denoting the superpotential of the MSSM without the μ -term, and λ , κ being the dimensionless parameters that describe the interactions among the superfields. When the singlet field \hat{S} develops a vacuum expectation value s , an effective μ is generated with $\mu_{eff} \equiv \lambda s$. The inclusion of the \hat{S} allows an additional contribution proportional to λ^2 to the Higgs potential, which will enhance the tree-level Higgs mass and reduce fine-tuning [24]. Traditionally, many studies focused on $\lambda \lesssim 0.7$, where the theory remains perturbative up to the grand unification scale (10^{16} GeV). In this scenario, the size of the additional contribution to the Higgs mass is restricted so that the issue of naturalness for 125 GeV Higgs is only partially addressed. In order to further reduce fine-tuning, the NMSSM with a relatively large λ around one (dubbed as λ -SUSY) is emphasized [25–32].

Due to the peculiarity of λ -SUSY theory, it may easily elevate the tree-level mass of the SM-like Higgs boson (denoted by h hereafter) larger than 125 GeV. So the structure of this boson must be a mixture of containing sizable singlet and/or non-SM doublet components [28–30], which induces the couplings of SM-like Higgs boson may deviate remarkably from

SM predictions. Moreover, the SM-like Higgs pair production in λ -SUSY may be enhanced significantly due to large trilinear self coupling of SM-like Higgs boson, which plays an indispensable role in constructing the Higgs potential.

Motivated by these arguments, we firstly study some features of the Higgs sector in λ -SUSY by considering various experimental constraints same as in work [23], then we explore the properties of h and the heaviest CP-even Higgs boson. Moreover, we also investigate the SM-like Higgs pair production and compare the results in λ -SUSY with the SM predictions. We ignore the lightest CP-even Higgs boson for its little contribution to the SM-like Higgs pair production because it mainly consists of the singlet field S for the surviving samples in this work.

The paper is organized as follows. In section II, we describe the features of the Higgs sector in λ -SUSY. In section III, we scan the parameter space of λ -SUSY by considering various theoretical and experimental constraints. Then in the allowed parameter space, we study the properties of SM-like Higgs boson h and the heaviest CP-even Higgs boson h_3 , and also investigate the pair production rates of h normalized to its SM prediction. Finally, in section IV, the conclusions are given.

II. HIGGS SECTOR IN λ -SUSY

In λ -SUSY theory, the scalar potential of the Higgs fields H_u , H_d and S consists of the contributions from the usual F-term and D-term, and also the soft breaking terms, which are given by:

$$V_{soft}^{NMSSM} = \tilde{m}_u^2 |H_u|^2 + \tilde{m}_d^2 |H_d|^2 + \tilde{m}_S^2 |S|^2 + (\lambda A_\lambda S H_u \cdot H_d + \frac{1}{3} \kappa A_\kappa \hat{S}^3 + h.c.). \quad (2)$$

Therefore, the Higgs sector Lagrangian includes 7 free parameters:

$$p_i^{susy} = \{\lambda, \kappa, \tilde{m}_u^2, \tilde{m}_d^2, \tilde{m}_S^2, A_\lambda, A_\kappa\}. \quad (3)$$

Like the general treatment of the multiple-Higgs theory, the Higgs fields of NMSSM can be written as follows:

$$H_u = \begin{pmatrix} H_u^+ \\ v_u + \frac{\varphi_u + i\phi_u}{\sqrt{2}} \end{pmatrix}, \quad H_d = \begin{pmatrix} v_d + \frac{\varphi_d + i\phi_d}{\sqrt{2}} \\ H_d^- \end{pmatrix}, \quad S = s + \frac{1}{\sqrt{2}}(\sigma + i\xi) \quad (4)$$

with v_u , v_d and s representing the vacuum expectation values of the fields H_u , H_d and S , respectively. However, in order to clearly see the Higgs particle implication on the LHC results, one usually rewrite the Higgs fields with one of them corresponds to the SM Higgs field [33],

$$H_1 = \begin{pmatrix} H^+ \\ \frac{S_1 + iP_1}{\sqrt{2}} \end{pmatrix}, \quad H_2 = \begin{pmatrix} G^+ \\ v + \frac{S_2 + iG^0}{\sqrt{2}} \end{pmatrix}, \quad H_3 = s + \frac{1}{\sqrt{2}}(S_3 + iP_2). \quad (5)$$

where

$$H_1 = \cos \beta H_u + \varepsilon \sin \beta H_d^*, \quad H_2 = \sin \beta H_u - \varepsilon \cos \beta H_d^*, \quad H_3 = S, \quad (6)$$

with $\varepsilon_{12} = -\varepsilon_{21} = 1$, $\varepsilon_{11} = \varepsilon_{22} = 0$, $\tan \beta \equiv v_u/v_d$ and $v = \sqrt{v_u^2 + v_d^2}$. Eq.(5) indicates that the Higgs sector of the NMSSM contains three physical CP-even Higgs bosons formed by the fields S_1 , S_2 and S_3 , two physical CP-odd Higgs bosons formed by the fields P_1 and P_2 , as well as one charged Higgs H^+ .

Through the minimization conditions of the scalar potential, the soft breaking parameters \tilde{m}_u^2 , \tilde{m}_d^2 , \tilde{m}_S^2 in Eq.(3) can be expressed in terms of m_Z , $\tan \beta$ and μ_{eff} . Therefore, the Higgs sector Lagrangian can also be described by the following six parameters,

$$\lambda, \quad \kappa, \quad \tan \beta, \quad \mu \equiv \lambda s, \quad M_A, M_P \quad (7)$$

with $M_A^2 = \frac{2\mu(A_\lambda + \kappa s)}{\sin 2\beta}$ and $M_P^2 = \lambda^2 v^2 \left(\frac{M_A \sin 2\beta}{2\mu}\right)^2 + \frac{3}{2}\lambda\kappa v^2 \sin 2\beta - 3\kappa s A_\kappa$ representing the squared masses of the CP-odd fields P_1 and P_2 , respectively. For the CP-even Higgs bosons in the basis(S_1, S_2, S_3), the mass matrix is given by [21, 22]

$$\begin{aligned} \mathcal{M}_{S,11}^2 &= M_A^2 + (m_Z^2 - \lambda^2 v^2) \sin^2 2\beta, \\ \mathcal{M}_{S,12}^2 &= -\frac{1}{2}(m_Z^2 - \lambda^2 v^2) \sin 4\beta, \\ \mathcal{M}_{S,13}^2 &= -\left(\frac{M_A^2 \sin 2\beta}{2\mu} + \kappa v_s\right) \lambda v \cos 2\beta, \\ \mathcal{M}_{S,22}^2 &= m_Z^2 \cos^2 2\beta + \lambda^2 v^2 \sin^2 2\beta, \\ \mathcal{M}_{S,23}^2 &= \left[1 - \left(\frac{M_A \sin 2\beta}{2\mu}\right)^2 - \frac{\kappa \sin 2\beta}{2\lambda}\right] 2\lambda\mu v, \\ \mathcal{M}_{S,33}^2 &= \frac{1}{6}\lambda^2 v^2 \left(\frac{M_A \sin 2\beta}{\mu}\right)^2 + 4(\kappa v_s)^2 - \frac{1}{3}M_P^2. \end{aligned} \quad (8)$$

By diagonalizing the mass matrix for CP-even Higgs bosons in the basis (S_1, S_2, S_3), one can obtain the corresponding mass eigenstates $h_i (i = 1, 2, 3)$:

$$h_i = \sum_{j=1}^3 V_{ij} S_j, \quad (9)$$

with V_{ij} denoting the rotation matrix and $m_{h_1} < m_{h_2} < m_{h_3}$. The state h_i with $|V_{i2}|^2 > 0.5$ is called the SM-like Higgs boson (labeled as h) and h_i with $|V_{i1}|^2 > 0.5$ is called non-SM doublet Higgs boson. Moreover, we define $\bar{S}_i = V_{i3}$, $\bar{D}_i = V_{i1}$, and they conform to the following sum rules

$$\bar{D}_1^2 + \bar{D}_2^2 + \bar{D}_3^2 = 1, \quad \bar{S}_1^2 + \bar{S}_2^2 + \bar{S}_3^2 = 1. \quad (10)$$

Obviously, $|\bar{S}_i|^2$ represents the singlet component of the physical state h_i and $|\bar{D}_i|^2$ represents the non-SM doublet component of h_i .

In the NMSSM, without the mixing among the states S_i , the mass of the SM-like Higgs boson h at tree level is given by

$$m_{h,tree}^2 \simeq m_Z^2 \cos^2 2\beta + \lambda^2 v^2 \sin^2 2\beta, \quad (11)$$

where the second term on the right side is additional contribution originating from the coupling $\lambda \hat{H}_u \cdot \hat{H}_d \hat{S}$ in the superpotential. Eq.(11) indicates that $m_{h,tree}$ can reach 125 GeV with a large λ around one, which may be realized in the so-called λ -SUSY theory [25, 26]. λ -SUSY theory is only an effective lagrangian at the weak scale and restricted to remain perturbative up to about 10 TeV, which renders the parameters λ and κ at weak scale satisfying the following relation [25]

$$0.17\lambda^2 + 0.26\kappa^2 \lesssim 1. \quad (12)$$

In order to measure the naturalness of the λ -SUSY theory, two fine tuning quantities are defined as follows [25, 34]:

$$\Delta_Z = \max_i \left| \frac{\partial \log m_Z^2}{\partial \log p_i} \right|, \quad \Delta_h = \max_i \left| \frac{\partial \log m_h^2}{\partial \log p_i} \right|, \quad (13)$$

where p_i includes the SUSY parameters at the weak scale listed in Eq.(3) and also top quark Yukawa coupling Y_t . We adopt the formulae presented in [34] and [25] to calculate Δ_Z and Δ_h . Obviously, with smaller values of Δ_Z and Δ_h , the λ -SUSY theory is more natural in predicting m_Z and m_h . Therefore, we use Δ_Z and Δ_h to estimate the goodness of the surviving samples and take $\max\{\Delta_Z, \Delta_h\} \leq 50$ as a criterion for naturalness.

In the following discussions, we only consider the scenario in which the next-to-lightest CP-even Higgs boson is SM-like Higgs boson h , and compare the results with work [23], which takes the lightest CP-even Higgs boson as the SM-like Higgs boson.

III. NUMERICAL RESULTS AND DISCUSSIONS

In this work we use the package NMSSMTools-4.0.0 to scan over the parameter space of λ -SUSY by considering various experimental and theoretical constraints,

$$\begin{aligned}
0.7 < \lambda \leq 2, \quad 0 < \kappa \leq 2, \quad 100 \text{ GeV} < M_A, M_P, \mu \leq 3 \text{ TeV}, \\
100 \text{ GeV} \leq M_{Q_3}, M_{U_3} \leq 2 \text{ TeV}, \quad |A_t| \leq 5 \text{ TeV}, \\
100 \text{ GeV} \leq m_{\tilde{t}}, M_2 \leq 1 \text{ TeV}, \quad 1 \leq \tan \beta \leq 15,
\end{aligned}
\tag{14}$$

with all the parameters defined at the 1TeV scale. Most of the constraints are implemented in the package NMSSMTools. Furthermore, we take $120 \text{ GeV} \leq m_h \leq 130 \text{ GeV}$ and consider the indirect constraints from the electroweak precision data, which strongly affect $\tan \beta$ in λ -SUSY.

For the surviving samples, we also perform a fit to the Higgs data from ATLAS [35], CMS [36] and CDF+D0 [37], and adopt the method introduced in [38, 39] to calculate corresponding χ^2 . We obtain $\chi^2_{min} = 11.7$ with Higgs data in 2014. In the following discussions, we consider three types of surviving samples and focus on samples with $\chi^2 \leq 25$, which corresponds to the samples consistent with the Higgs data at 95% C.L..

- Type-I samples: samples satisfying both $\chi^2 \leq 25$ and $\max\{\Delta_Z, \Delta_h\} \leq 50$, which are regarded as the physical samples in our discussion.
- Type-II samples: samples satisfying both $\chi^2 \leq 25$ and $\max\{\Delta_Z, \Delta_h\} > 50$, which coincide with the experiments but are not favored by the fine tuning argument.
- Type-III samples: samples satisfying $\chi^2 > 25$, which are of less interest than the previous two types.

Since the λ -SUSY theory is more natural in predicting m_Z and m_h than the MSSM, we display the characters of Δ_Z and Δ_h in λ -SUSY. In fig.1 we show the surviving samples on the plane of μ versus λ with the corresponding values of Δ_Z and Δ_h in different colors. The figure manifests that the largest value of λ may reach to 1.1, which is different from the scenario with the lightest CP-even Higgs boson as the SM-like Higgs boson, in which the value of λ can reach to 1.8 [23]. This is because the mixing of the fields S_2 and S_3 can push up the SM-like Higgs boson mass when the next-to-lightest CP-even Higgs boson is SM-like.

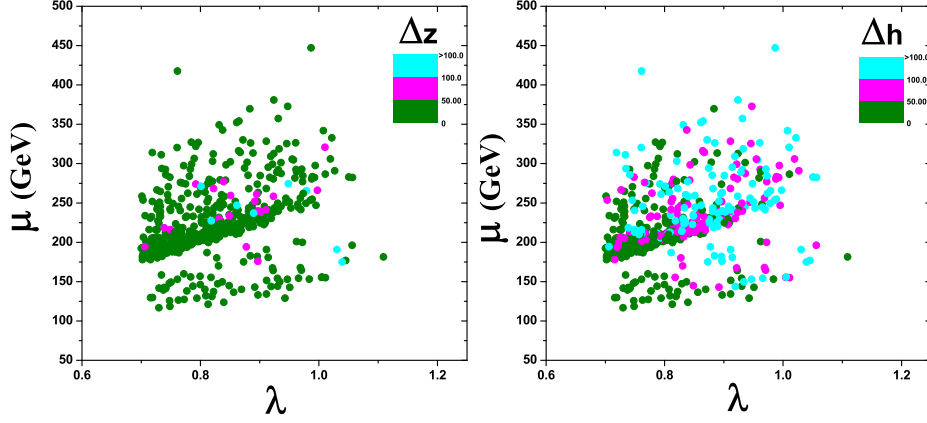


FIG. 1: Surviving samples satisfying $\chi^2 \leq 25$, projected on the plane of μ versus λ . For these samples, their corresponding values of Δ_Z and Δ_h are displayed with different colors.

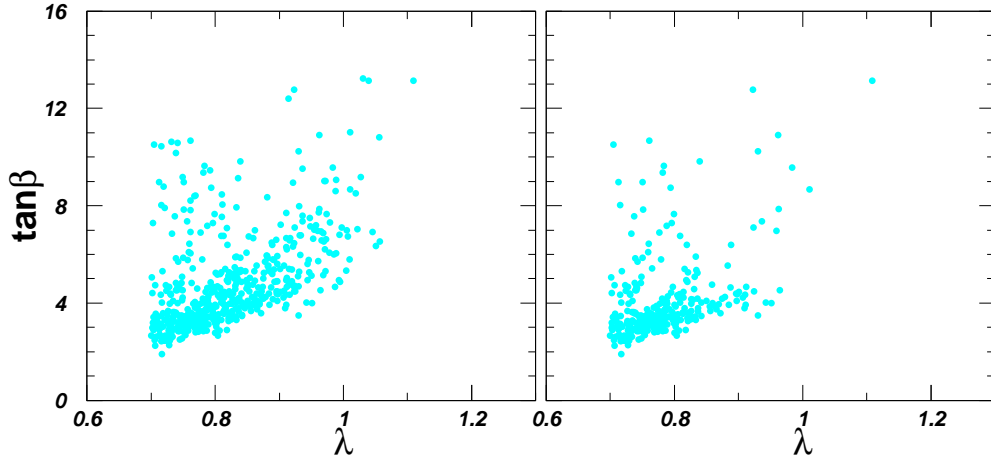


FIG. 2: Surviving samples satisfying $\chi^2 \leq 25$, projected on the plane of $\tan\beta$ versus λ . Samples in the right panel are further required to satisfy $\max\{\Delta_Z, \Delta_h\} \leq 50$.

Due to the important role of $\tan\beta$ and λ in λ -SUSY, we show the correlation between them in Fig. 2. The surviving samples satisfy $\chi^2 \leq 25$ and those in the right panel are further required to satisfy $\max\{\Delta_Z, \Delta_h\} \leq 50$. The figure indicates that $\tan\beta$ tends to increase with the increase of λ and some samples with relatively small values of $\tan\beta$ are excluded after requiring $\max\{\Delta_Z, \Delta_h\} \leq 50$. This is because a large value of $\tan\beta$ can reduce the tree level Higgs boson mass $m_{h,tree}$, which is able to cancel out the mixing effect of the fields S_2 and S_3 in order to obtain a 125 GeV Higgs boson.

In the following discussions, we investigate the properties of the next-to-lightest and

heaviest CP-even Higgs bosons for the above three types of samples. We pay particular attention to the features of these bosons that differentiate from [23].

A. Properties of the Next-to-Lightest CP-even Higgs Boson h_2

Throughout this work we take the next-to-lightest CP-even Higgs boson h_2 as the SM-like Higgs boson h , so in the following discussions, we explore the features of this boson and also its coupling information.

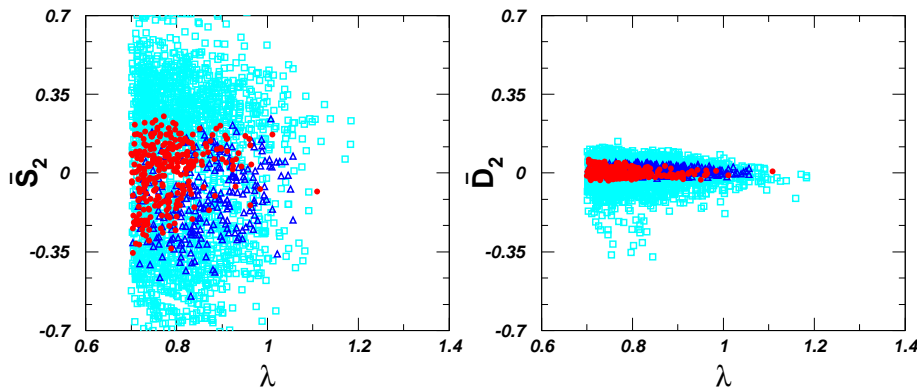


FIG. 3: Singlet component coefficient \bar{S}_2 and non-SM doublet component coefficient \bar{D}_2 of the SM-like Higgs boson as a function of λ for Type-I sample (red bullet), Type-II sample (blue triangle) and Type-III sample (sky-blue square).

In Fig.3, we project the three types of surviving samples on the plane of $\bar{S}_2 - \lambda$ and $\bar{D}_2 - \lambda$, where \bar{S}_2 and \bar{D}_2 denote the singlet component coefficient and non-SM doublet component coefficient of h respectively. The figure shows that the range of the values of $|\bar{S}_2|$ is always larger than that of $|\bar{D}_2|$. As is showed in Fig.3, $|\bar{S}_2|$ may exceed 0.7 and be smaller than 0.35 before and after considering the Higgs data at 95% C.L. respectively. In comparison, $|\bar{D}_2|$ reaches maximally about 0.35, and it is less than 0.1 with the Higgs data at 95% C.L.. This is because the constraints we considered have put weak restrictions on the element $\mathcal{M}_{S,33}^2$ of the CP-even Higgs mass matrix due to the singlet nature of the field S_3 . Compared with the Figure 3 in [23], we find the values of the singlet component coefficient $|\bar{S}_2|$ has a wider range in our discussion than in the work [23], which take the lightest CP-even Higgs boson as the SM-like Higgs boson. The reason is that $m_{h,tree}$ will be easily lifted to much larger than 125 GeV and the sizable singlet component can effectively pull down the mass.

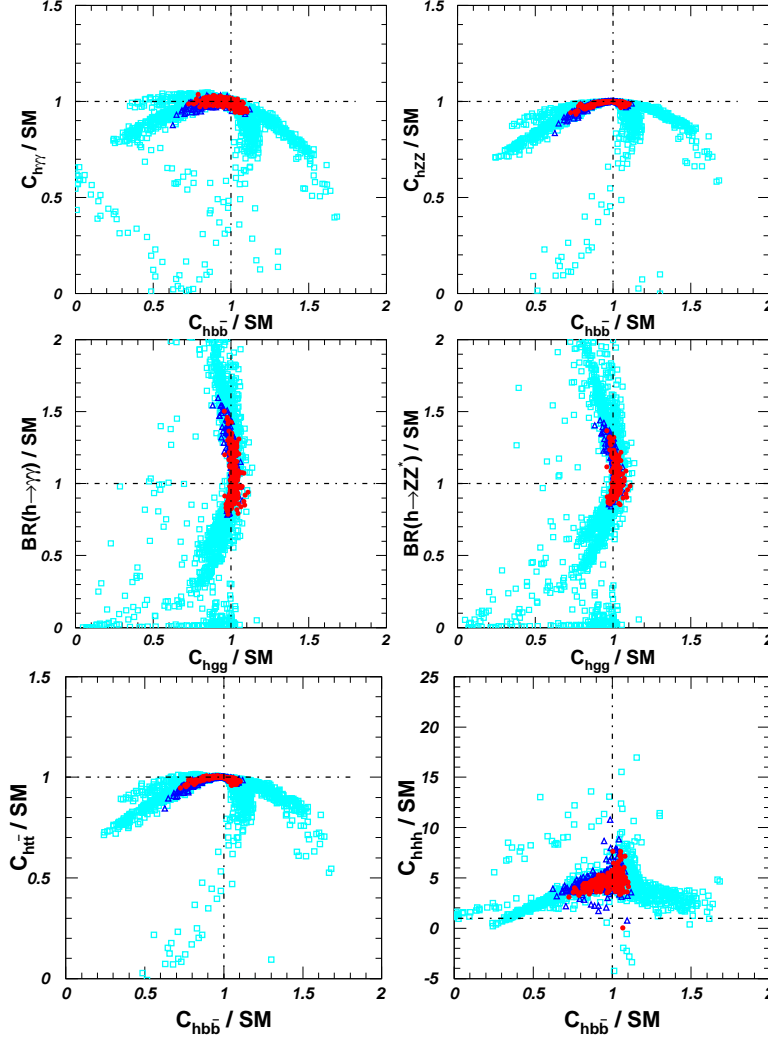


FIG. 4: Same as Fig.3, but showing the coupling information of the SM-like Higgs boson h .

In Fig.4, we exhibit the coupling information of h . This figure indicates that, after considering the Higgs data at 95% C.L., the normalized couplings $C_{h\gamma\gamma}/SM$, C_{hZZ}/SM , C_{hgg}/SM and $C_{h\tau\tau}/SM$ are limited within 20% deviation from unity, and the couplings $C_{hb\bar{b}}/SM$ are allowed to vary in relatively wider ranges, at 40% deviating from unity. The normalized branching ratios $Br(h \rightarrow \gamma\gamma)/SM$ and $Br(h \rightarrow ZZ)/SM$ may vary from 0.8 to 1.5. For the Higgs triple self coupling C_{hhh}/SM , the right panel of the last row in Fig.4 indicates that it can only reach 7 and 10 for the Type-I samples and Type-II samples respectively.

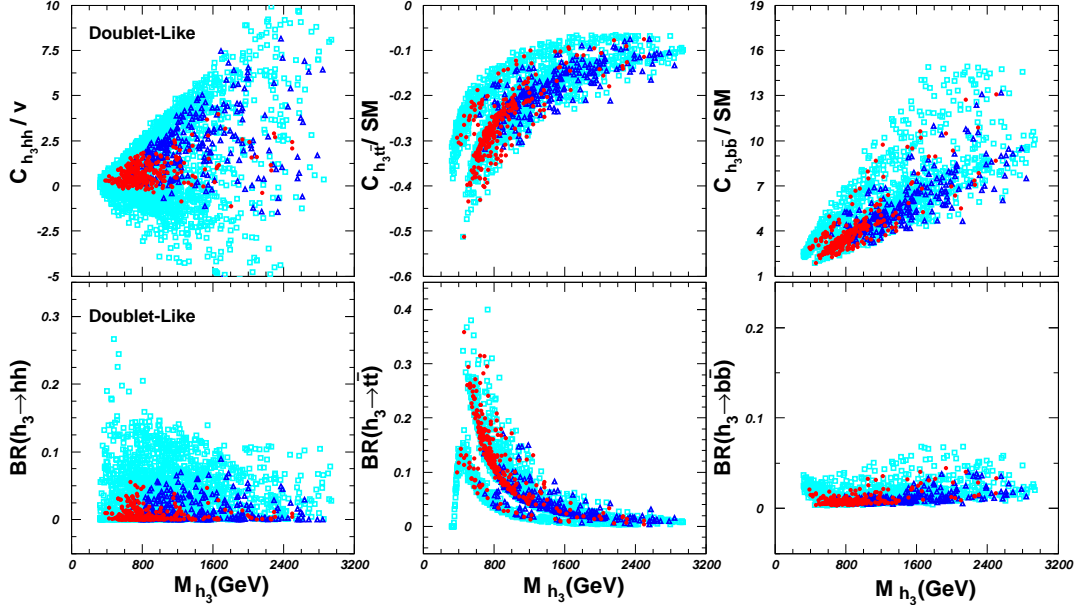


FIG. 5: Same as Fig.3, but showing the couplings and branching ratios of doublet dominated h_3 as a function of M_{h_3} .

B. Properties of the heaviest CP-even Higgs Boson h_3

We here simply study the properties of the heaviest CP-even Higgs boson h_3 . We find that the non-SM doublet component coefficient \bar{D}_3^2 of h_3 is over 0.9 for Type-I and Type-II samples, that is to say, h_3 is dominated by the non-SM doublet, which can be foreordained.

In Fig.5, we show the normalized couplings of the h_3 such as C_{h_3hh}/v , $C_{h_3\bar{t}t}/SM$ and $C_{h_3\bar{b}b}/SM$ as functions of M_{h_3} and also plot the branching ratios of $h_3 \rightarrow hh$, $h_3 \rightarrow \bar{t}t$ and $h_3 \rightarrow \bar{b}b$. We can learn the following features from Fig.5: (1) For all the surviving samples, $m_{h_3} \gtrsim 400$ GeV; (2) The normalized coupling C_{h_3hh}/v may still be large with the maximum value reaching 5, and $C_{h_3\bar{b}b}/SM$ is larger than 1 with maximum value of 10 in optimal case. While for the normalized coupling $C_{h_3\bar{t}t}/SM$, it is smaller than 1 and $0.2 \leq |C_{h_3\bar{t}t}/SM| \leq 0.4$. (3) For $500 \text{ GeV} \leq m_{h_3} \leq 1000 \text{ GeV}$, $h_3 \rightarrow \bar{t}t$ may act as the dominant decay channel of h_3 .

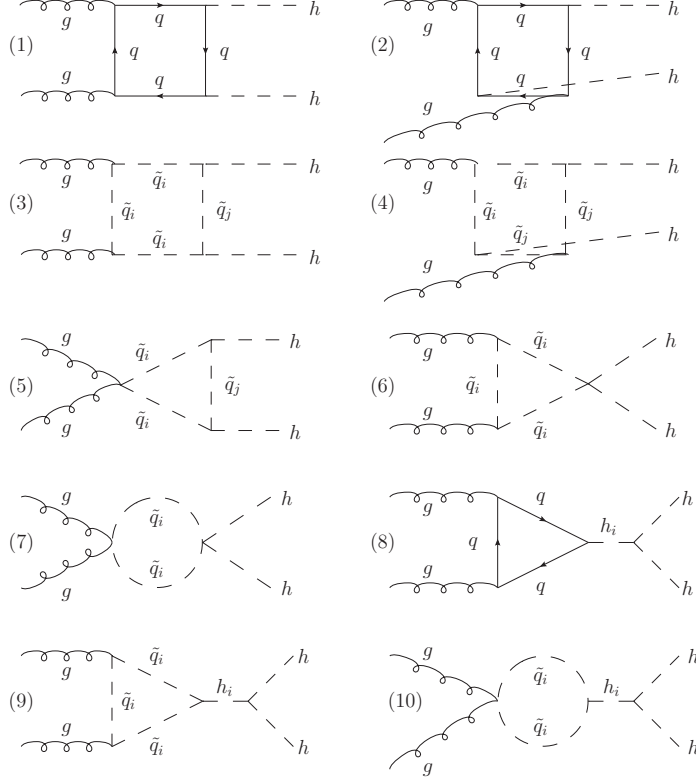


FIG. 6: Feynman diagrams for the pair production of the SM-like Higgs boson via gluon fusion in λ -SUSY with h_i denoting a CP-even Higgs ($i = 1, 2, 3$) and $\tilde{q}_{i,j}$ ($i, j = 1, 2$) denoting a squark. The diagrams with initial gluons or final Higgs bosons interchanged are not shown here.

C. Higgs Pair Production at the LHC

As a rare process at the LHC compared with other Higgs production channels, the Higgs pair production plays a significant role in extracting Higgs self interaction C_{hhh} , which is indispensable to reconstruct the Higgs potential and finally interpret the mechanism of the electroweak symmetry breaking [40–43]. So the studies on the Higgs pair production in λ -SUSY should be carefully investigated.

In SUSY, the Higgs pair production may proceed through the diagrams (1)-(10) in Fig.6 [44–46], where the diagrams with initial gluons or final Higgs bosons interchanged are not shown, and we only consider the contributions from the third generation quarks and squarks due to their large Yukawa couplings. The SUSY prediction on the production rate may significantly deviate from the SM prediction because the contribution to the amplitude from SUSY is of the same perturbation order as that from the SM. Based on previous studies in

the SUSY [47–51], we learn that the Higgs pair production rate may significantly enhanced mainly through the following three mechanisms: (i)Through the loops mediated by stops [47]. The major contributions come from diagrams (3)-(5) of Fig.6, and the quantitative amplitude can be given by $\mathcal{M} \sim \alpha_s^2 Y_t^2 \left(c_1 \sin^2 2\theta_t \frac{A_t^2}{m_{\tilde{t}_1}^2} + c_2 \frac{A_t^2}{m_{\tilde{t}_2}^2} \right)$ with θ_t being the mixing angle of stops and c_1, c_2 denoting dimensionless coefficients; (ii)Through large Higgs self coupling [48]; (iii)Through the resonant effect of h_i [49–51]. In this work, only the heaviest CP-even Higgs h_3 can be on-shell produced by gg or $b\bar{b}$ initial state.

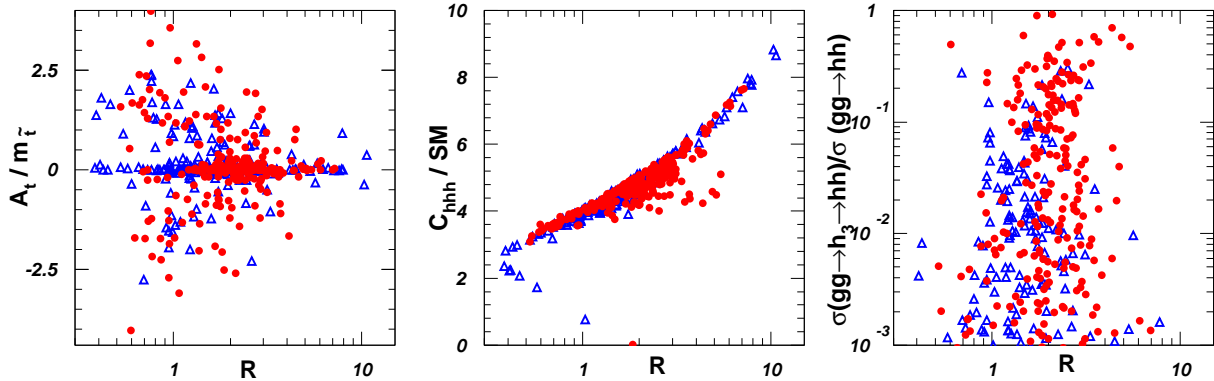


FIG. 7: The scatter plots of the Type-I samples (red bullet) and Type-II samples (blue triangle), showing $A_t/m_{\tilde{t}}$, C_{hhh}/SM and the pure resonant s-channel contribution to the pair production as a function of R in left panel, middle panel and right panel respectively.

In order to investigate which mechanism is to mainly enhance the Higgs pair production rate, in fig.7 we present $A_t/m_{\tilde{t}}$, C_{hhh}/SM , the pure resonant s-channel contribution to the pair production as a function of the normalized Higgs pair production rate R , where $R = \sigma(pp \rightarrow hh)/(\sigma_{SM}^{LO}(PP \rightarrow hh)|_{m_h=125 \text{ GeV}}) \simeq \sigma(pp \rightarrow hh)/(19fb)$. The figure shows that the Higgs pair production rate can be enhanced by about 10 times maximally and the main contributions come from the Higgs self coupling. In comparison with the scenario of the lightest Higgs boson as SM-like Higgs in work [23], the enhancement of the Higgs pair production rate is un conspicuous. The main reason is, as the right panel of the last row in Fig.4 shows, that the enhancement of the Higgs triple self coupling C_{hhh}/SM are less significant than that in [23]. In addition, the maximum value of the normalized Higgs pair production rate is roughly same with the case in NMSSM with $\lambda < 0.7$ [47], where the enhancement is mainly through the loops mediated by stops.

IV. CONCLUSION

In this work, we investigate the properties of the SM-like Higgs boson in λ -SUSY theory, which corresponds to the NMSSM with a large λ around one. Throughout this work, we treat the next-to-lightest CP-even Higgs boson as the SM-like Higgs boson. To make our study realistic, we firstly define quantities Δ_Z and Δ_h to measure the naturalness of the parameter points and consider the Higgs data at 95% C.L.. Then we implement various experimental constraints on the parameter space of λ -SUSY. In the allowed parameter space, we investigate features of the SM-like Higgs boson and the heaviest CP-even Higgs boson, and also study the pair production of the SM-like Higgs boson. As is shown in this work, we find the following features:

- Considering the naturalness argument, λ is less than 1.1. However, λ can reach 1.8 in work [23], which treats the lightest CP-even Higgs boson as the SM-like Higgs boson. Moreover, after considering the naturalness argument, the surviving samples are fewer, especially Δ_h plays more important role in selecting the parameter space of λ -SUSY.
- Same as the current conclusion in [23], Higgs data at 95% C.L. still allow for a sizable singlet component in h , which at most reaches 35%, while the non-SM doublet component is forbidden to be larger than 10%.
- The strength of the triple self coupling of h can only reach 7 and 10 for the Type-I samples and Type-II samples respectively, which is smaller than the maximum value in work [23].
- The heaviest CP-even Higgs boson h_3 is highly non-SM doublet dominated and its mass may be as light as 400 GeV. For $500 \text{ GeV} \leq m_{h_3} \leq 1000 \text{ GeV}$, $h_3 \rightarrow \bar{t}t$ may act as the dominant decay channel.
- In most cases the dominant contribution to the Higgs pair production comes from the triple self coupling of the Higgs boson and the production rate can be greatly enhanced, maximally 10 times larger than the SM prediction.

Acknowledgement

We thank Prof. Junjie Cao for helpful discussions. This work was supported in part by the National Natural Science Foundation of China (NNSFC) under grant No. 11305050, and by Specialized Research Fund for the Doctoral Program of Higher Education with grant No. 20124104120001.

-
- [1] G. Aad *et al.* [ATLAS Collaboration], Phys. Lett. B **716**, 1 (2012) [arXiv:1207.7214 [hep-ex]].
 - [2] S. Chatrchyan *et al.* [CMS Collaboration], Phys. Lett. B **716**, 30 (2012) [arXiv:1207.7235 [hep-ex]].
 - [3] [ATLAS Collaboration], ATLAS-CONF-2013-034, ATLAS-COM-CONF-2013-035.
 - [4] [CMS Collaboration], CMS-PAS-HIG-13-005.
 - [5] G. Aad *et al.*, [ATLAS Collaboration], Phys. Lett. B **716**, 1 (2012); S. Chatrchyan *et al.*, [CMS Collaboration], Phys. Lett. B **716**, 30 (2012).
 - [6] The ATLAS Collaboration ATLAS-CONF-2012-170; The CMS Collaboration CMS-PAS-HIG-12-045.
 - [7] S. Heinemeyer, O. Stal and G. Weiglein, Phys. Lett. B **710**, 201 (2012) [arXiv:1112.3026 [hep-ph]].
 - [8] P. Draper, P. Meade, M. Reece and D. Shih, Phys. Rev. D **85**, 095007 (2012) [arXiv:1112.3068 [hep-ph]].
 - [9] M. Carena, S. Gori, N. R. Shah and C. E. M. Wagner, JHEP **1203**, 014 (2012) [arXiv:1112.3336 [hep-ph]].
 - [10] J. Cao, Z. Heng, D. Li and J. M. Yang, Phys. Lett. B **710**, 665 (2012) [arXiv:1112.4391 [hep-ph]].
 - [11] N. D. Christensen, T. Han and S. Su, Phys. Rev. D **85**, 115018 (2012) [arXiv:1203.3207 [hep-ph]].
 - [12] U. Ellwanger, JHEP **1203**, 044 (2012) [arXiv:1112.3548 [hep-ph]].
 - [13] J. F. Gunion, Y. Jiang and S. Kraml, Phys. Lett. B **710**, 454 (2012) [arXiv:1201.0982 [hep-ph]].
 - [14] J. J. Cao, Z. X. Heng, J. M. Yang, Y. M. Zhang and J. Y. Zhu, JHEP **1203**, 086 (2012) [arXiv:1202.5821 [hep-ph]].

- [15] D. A. Vasquez, G. Belanger, C. Boehm, J. Da Silva, P. Richardson and C. Wymant, *Phys. Rev. D* **86**, 035023 (2012) [arXiv:1203.3446 [hep-ph]].
- [16] R. Benbrik, M. Gomez Bock, S. Heinemeyer, O. Stal, G. Weiglein and L. Zeune, *Eur. Phys. J. C* **72**, 2171 (2012) [arXiv:1207.1096 [hep-ph]].
- [17] K. Choi, S. H. Im, K. S. Jeong and M. Yamaguchi, *JHEP* **1302**, 090 (2013) [arXiv:1211.0875 [hep-ph]].
- [18] S. F. King, M. Mhleitner, R. Nevzorov and K. Walz, *Nucl. Phys. B* **870**, 323 (2013) [arXiv:1211.5074 [hep-ph]].
- [19] M. Badziak, M. Olechowski and S. Pokorski, *JHEP* **1306**, 043 (2013) [arXiv:1304.5437 [hep-ph]].
- [20] S. Moretti, S. Munir and P. Poulose, *Phys. Rev. D* **89**, no. 1, 015022 (2014) [arXiv:1305.0166 [hep-ph]].
- [21] U. Ellwanger, C. Hugonie and A. M. Teixeira, *Phys. Rept.* **496**, 1 (2010) [arXiv:0910.1785 [hep-ph]].
- [22] M. Maniatis, *Int. J. Mod. Phys. A* **25**, 3505 (2010) [arXiv:0906.0777 [hep-ph]].
- [23] J. Cao, D. Li, L. Shang, P. Wu and Y. Zhang, *JHEP* **1412**, 026 (2014) [arXiv:1409.8431 [hep-ph]].
- [24] Z. Kang, J. Li and T. Li, *JHEP* **1211**, 024 (2012) [arXiv:1201.5305 [hep-ph]].
- [25] R. Barbieri, L. J. Hall, Y. Nomura and V. S. Rychkov, *Phys. Rev. D* **75**, 035007 (2007) [hep-ph/0607332].
- [26] J. Cao and J. M. Yang, *Phys. Rev. D* **78**, 115001 (2008) [arXiv:0810.0989 [hep-ph]].
- [27] M. Perelstein and B. Shakya, *Phys. Rev. D* **88**, no. 7, 075003 (2013) [arXiv:1208.0833 [hep-ph]].
- [28] L. J. Hall, D. Pinner and J. T. Ruderman, *JHEP* **1204**, 131 (2012) [arXiv:1112.2703 [hep-ph]].
- [29] K. Agashe, Y. Cui and R. Franceschini, *JHEP* **1302**, 031 (2013) [arXiv:1209.2115 [hep-ph]].
- [30] T. Gherghetta, B. von Harling, A. D. Medina and M. A. Schmidt, *JHEP* **1302**, 032 (2013) [arXiv:1212.5243 [hep-ph]].
- [31] R. Barbieri, D. Buttazzo, K. Kannike, F. Sala and A. Tesi, *Phys. Rev. D* **87**, no. 11, 115018 (2013) [arXiv:1304.3670 [hep-ph]].
- [32] M. Farina, M. Perelstein and B. Shakya, *JHEP* **1404**, 108 (2014) [arXiv:1310.0459 [hep-ph]].
- [33] U. Ellwanger, C. Hugonie and A. M. Teixeira, *Phys. Rept.* **496**, 1 (2010); M. Maniatis, *Int.*

- J.Mod. Phys. A25 (2010) 3505; S. F. King, P. L. White, Phys. Rev. D 52, 4183 (1995).
- [34] U. Ellwanger, G. Espitalier-Noel and C. Hugonie, JHEP **1109**, 105 (2011) [arXiv:1107.2472 [hep-ph]].
- [35] ATLAS collaboration, ATL-PHYS-PUB-2014-009 (2014).
- [36] CMS collaboration, CMS-PAS-HIG-14-009 (2014).
- [37] T. Aaltonen *et al.* [CDF and D0 Collaborations], Phys. Rev. D **88**, no. 5, 052014 (2013) [arXiv:1303.6346 [hep-ex]].
- [38] J. R. Espinosa, C. Grojean, M. Muhlleitner and M. Trott, JHEP **1205**, 097 (2012) [arXiv:1202.3697 [hep-ph]].
- [39] P. P. Giardino, K. Kannike, M. Raidal and A. Strumia, JHEP **1206**, 117 (2012) [arXiv:1203.4254 [hep-ph]].
- [40] M. J. Dolan, C. Englert and M. Spannowsky, JHEP **1210**, 112 (2012) [arXiv:1206.5001 [hep-ph]].
- [41] M. McCullough, Phys. Rev. D **90**, no. 1, 015001 (2014) [Phys. Rev. D **92**, no. 3, 039903 (2015)] [arXiv:1312.3322 [hep-ph]].
- [42] L. Wu, J. M. Yang, C. P. Yuan and M. Zhang, Phys. Lett. B **747**, 378 (2015) [arXiv:1504.06932 [hep-ph]].
- [43] Q. H. Cao, B. Yan, D. M. Zhang and H. Zhang, Phys. Lett. B **752**, 285 (2016) [arXiv:1508.06512 [hep-ph]].
- [44] D. T. Nhung, M. Muhlleitner, J. Streicher and K. Walz, JHEP **1311**, 181 (2013) [arXiv:1306.3926 [hep-ph]].
- [45] U. Ellwanger, JHEP **1308**, 077 (2013) [arXiv:1306.5541 [hep-ph]].
- [46] C. Han, X. Ji, L. Wu, P. Wu and J. M. Yang, JHEP **1404**, 003 (2014) [arXiv:1307.3790 [hep-ph]].
- [47] J. Cao, Z. Heng, L. Shang, P. Wan and J. M. Yang, JHEP **1304**, 134 (2013) [arXiv:1301.6437 [hep-ph]].
- [48] J. Cao, Y. He, P. Wu, M. Zhang and J. Zhu, JHEP **1401**, 150 (2014) [arXiv:1311.6661 [hep-ph]].
- [49] J. Liu, X. P. Wang and S. h. Zhu, arXiv:1310.3634 [hep-ph].
- [50] J. M. No and M. Ramsey-Musolf, Phys. Rev. D **89**, no. 9, 095031 (2014) [arXiv:1310.6035 [hep-ph]].

- [51] V. Barger, L. L. Everett, C. B. Jackson, A. D. Peterson and G. Shaughnessy, *Phys. Rev. Lett.* **114**, no. 1, 011801 (2015) [arXiv:1408.0003 [hep-ph]].